Nrf2 affects the efficiency of mitochondrial fatty acid oxidation

Marthe H. R. Ludtmann[*], **Plamena R. Angelova**[*], **Ying Zhang**[†], **Andrey Y. Abramov**[*,1], and **Albena T. Dinkova-Kostova**[†,‡,1]

[*]Department of Molecular Neuroscience, Institute of Neurology, University College London, London WC1N 3BG, U.K.

[†]Jacqui Wood Cancer Centre, Division of Cancer Research, Medical Research Institute, University of Dundee, Dundee DD1 9SY, U.K.

[‡]Department of Pharmacology and Molecular Sciences, Johns Hopkins University School of Medicine, Baltimore, MD 21205, U.S.A.

Abstract

Transcription factor Nrf2 (NF-E2 p45-related factor 2) regulates the cellular redox homoeostasis and cytoprotective responses, allowing adaptation and survival under conditions of stress. The significance of Nrf2 in intermediary metabolism is also beginning to be recognized. Thus this transcription factor negatively affects fatty acid synthesis. However, the effect of Nrf2 on fatty acid oxidation is currently unknown. In the present paper, we report that the mitochondrial oxidation of long-chain (palmitic) and short-chain (hexanoic) fatty acids is depressed in the absence of Nrf2 and accelerated when Nrf2 is constitutively active. Addition of fatty acids stimulates respiration in heart and liver mitochondria isolated from wild-type mice. This effect is significantly weaker when Nrf2 is deleted, whereas it is stronger when Nrf2 activity is constitutively high. In the absence of glucose, addition of fatty acids differentially affects the production of ATP in mouse embryonic fibroblasts from wild-type, Nrf2-knockout and Keap1 (Kelch-like ECH-associated protein 1)-knockout mice. In acute tissue slices, the rate of regeneration of $FADH_2$ is reduced when Nrf2 is absent. This metabolic role of Nrf2 on fatty acid oxidation has implications for chronic disease conditions including cancer, metabolic syndrome and neurodegeneration.

Keywords

ATP; FAD; fatty acid oxidation; Kelch-like ECH-associated protein 1 (Keap1); live-cell imaging; tissue slice

---

INTRODUCTION

The basic leucine zipper transcription factor Nrf2 (NF-E2 p45-related factor 2) and its repressor Keap1 (Kelch-like ECH-associated protein 1) regulate the expression of networks of genes encoding proteins with versatile cytoprotective functions [1]. Under homoeostatic conditions, Nrf2 binds to Keap1, which forms a RING E3-ubiquitin ligase with Cul (Cullin)-3/Rbx1 and continuously targets the transcription factor for ubiquitination and proteasomal degradation. In response to electrophiles and oxidants (termed inducers), which recognize and chemically modify specific cysteine residues of Keap1, ubiquitination of Nrf2 is inhibited; consequently, Nrf2 accumulates and activates transcription [2-5].

Among the cytoprotective Nrf2-dependent gene products, enzymes involved in the biosynthesis of reducing equivalents, such as NADPH, and molecules that are responsible for the maintenance of the redox homoeostasis, such as glutathione and thioredoxin, are especially prominent. Both the GCLC (catalytic γ-glutamyl cysteine ligase) and GCLM (regulatory γ-glutamyl cysteine ligase) subunits of GCL (γ-glutamyl cysteine ligase), the enzyme that catalyses the rate-limiting step in glutathione biosynthesis, are encoded by genes which are direct targets of Nrf2 [6]. Nrf2 is also involved in the generation of NADPH, by regulating the gene expression of ME-1 (malic enzyme 1), IDH-1 (isocitrate dehydrogenase 1), G6PD (glucose-6-phosphate dehydrogenase), and PGD (6-phosphogluconate dehydrogenase) [7-10]. In turn, NADPH provides the reducing equivalents needed for the maintenance of glutathione and thioredoxin in their reduced states through the catalytic power of glutathione reductase and thioredoxin reductase, both of which are products of Nrf2-target genes. Consequently, Nrf2-KO (knockout) cells have lower levels of glutathione, whereas Keap1 deficiency leads to glutathione up-regulation [11,12]. In full agreement with these alterations in the biosynthesis and regeneration of glutathione, the principal small molecule antioxidant in the cell, the levels of ROS (reactive oxygen species) are increased under conditions of Nrf2 deficiency. Conversely, constitutive genetic or pharmacological activation of the transcription factor lowers ROS production [12,13].

The role of glutathione and ROS in the most basic cellular processes, such as energy metabolism, is increasingly being recognized. Thus KD (knockdown) of G6PD increases the levels of ROS while decreasing the levels of ATP, and this ROS-mediated inhibition of ATP production correlates with down-regulation of mitochondrial FAO (fatty acid oxidation) [14]. Both acute and chronic glutathione deficiency, such as that observed during aging, promotes impaired FAO and glutathione restoration reverses this effect [15]. Curiously, Nrf2 not only controls the intracellular levels of glutathione and ROS, it also negatively regulates lipid biosynthesis: the hepatic mRNA levels of ATP-citrate lyase, fatty acid synthase and stearoyl CoA desaturase, three critical enzymes involved in FAS (fatty acid synthesis), are down-regulated by both genetic (by Keap1-KO) and pharmacological {by the semi-synthetic potent inducer oleanane triterpenoid 1-[2-cyano-3,12-dioxooleana-1,9(11)-dien-28-oyl]imidazole} activation of the transcription factor [16]. These findings are consistent with the observed increase in lipid accumulation in the livers of Nrf2-KO mice in comparison with WT (wild-type) animals, most notably in nutritional models of non-alcoholic steatohepatitis [17,18]. Proteomics and immunoblotting analysis have shown that

the levels of ATP-citrate lyase, the catalytic action of which provides acetyl-CoA for FAS, are higher in livers of Nrf2-KO mice in comparison with their WT counterparts [19]. Acetyl-CoA serves as a precursor for FAS via its conversion into malonyl-CoA which, in turn, is committed to FAS by its involvement in the elongation of fatty acids through the enzyme activity of fatty acid synthase. In addition to stimulating FAS, malonyl-CoA inhibits FAO by allosteric inhibition of CPT1 (carnitine palmitoyltransferase 1), an outer mitochondrial membrane enzyme which conjugates long-chain fatty acids with carnitine, thus allowing their translocation into the mitochondria, where they undergo FAO.

Similar to the down-regulation of ATP-citrate lyase, the reduced expression of stearoyl CoA desaturase under conditions of constitutive activation of Nrf2 is also expected to lower FAS as this enzyme catalyses the biosynthesis of mono-unsaturated fatty acids, giving rise to palmitoleic acid and oleic acid, key substrates for the formation of complex lipids such as phospholipids, triglycerides, cholesterol esters and alkyl-2,3-diacylglycerols. Indeed, mice deficient in stearoyl CoA desaturase exhibit reduced FAS and enhanced FAO [20]. Conversely, compared with WT animals, Nrf2-KO mice have a higher hepatic expression of stearoyl-CoA desaturase, correlating with higher triglyceride levels [21].

In contrast with these well-documented effects on FAS, to our knowledge, the potential role of Nrf2 in FAO, has not been examined previously. Mitochondrial FAO provides the majority (80–90%) of the total fatty acid-derived energy [22]. Dysregulation in FAO contributes to the pathogenesis of human disease and aging. The significance of altered FAO in cancer metabolism is well recognized, both in terms of ATP production, as well as a source of NADPH which is used to counteract oxidative stress that is necessary for cancer cell survival, and in anabolic reactions which provide building blocks to sustain cell growth and proliferation [23]. Thus inefficient FAO and mitochondrial dysfunction will increase ROS generation and may cause DNA damage and facilitate tumour initiation. However, increased FAO may also contribute to tumour growth by providing sources of energy (ATP) and reducing equivalents (NADPH). Given the reciprocal relationship between FAS and FAO, the negative regulation of the gene expression of multiple enzymes involved in FAS by Nrf2, and its function in cellular redox homoeostasis and NADPH generation and utilization, we hypothesized that the activity of the leucine zipper transcription factor may influence the efficiency of FAO. We tested this hypothesis by the use of cells, intact mitochondria and live-cell imaging of acute tissue slices isolated from mice in which Nrf2 is either genetically deleted or constitutively activated, and comparing them with their WT counterparts.

MATERIALS AND METHODS

Animals and cells

WT, Nrf2-KO and Keap1-KD C57BL/6 mice were maintained on a 12 h light/12 h dark cycle, 35% humidity, with free access to water and food (pelleted RM1 diet from SDS Special Diets Services). The Nrf2-KO mice, originally created by Itoh et al. [24] and kindly provided by Dr Ken Itoh and Professor Masayuki Yamamoto (Department of Medical Biochemistry, Tohoku University, Japan), were backcrossed over six generations on to a C57BL/6 background in our animal facility as described previously [25]. The Keap1-KD

(Keap1$^{flox/flox}$) C57BL/6 mice [26] were also generated and kindly provided by Professor Masayuki Yamamoto. Breeding and maintenance were strictly compliant with the U.K. Animals (Scientific Procedures) Act 1986.

MEFs (mouse embryonic fibroblasts) isolated from pools of WT, Keap1-KO and Nrf2-KO 13.5-day-old mouse embryos derived from two- to three-time-pregnant female mice [27,28] were maintained at 37°C in a humidified atmosphere of 5% CO_2 and 95% air in dishes coated for 30 min with 0.1% gelatin. Cells were grown in Iscove's modified Dulbecco's medium (with L-glutamine), supplemented with 10% (v/v) heat-inactivated FBS, insulin–transferrin–selenium and 10 ng/ml epidermal growth factor (Gibco, Invitrogen).

The levels of Nrf2 in the three genotypes of MEFs were confirmed by immunoblotting using a rabbit polyclonal antibody (a gift from Professor John D. Hayes, Division of Cancer Research, Medical Research Institute, University of Dundee) at a dilution of 1:2000 [29] and anti-β-actin mouse monoclonal antibody (1:10000 dilution, Sigma) as a loading control. The enzyme activity of NQO1 [NAD(P)H:quinone oxidoreductase 1] was measured in cell lysates using menadione as a substrate as described previously [30]. ATP levels were determined 24 h post-transfection with the ATP biosensor AT1.03 [31] using Effectene (Qiagen).

Preparation of acute heart slices

Transverse acute heart slices (~100 μm) were prepared from the left ventricle of 34–50-week-old female WT, Nrf2-KO and Keap1-KD C57BL/6 mice. The animals were killed by cervical dislocation, their hearts were collected and the heart tissue was immediately sliced at 4°C using a vibratome (Leica VT1000S). The tissue slices were maintained in 10 mM BDM (2,3-butanedione monoxime)-supplemented physiological saline at room temperature (24°C) for ~1 h before imaging.

Live-cell imaging

Confocal images were obtained using a Zeiss 710 VIS (visible) CLSM microscope equipped with a META detection system and a ×40 oil immersion objective. The FAD autofluorescence was determined using 458 nm Argon laser line and fluorescence was measured from 505 to 550 nm. Illumination intensity was kept to a minimum (at 0.1–0.2% of laser output) to avoid phototoxicity, and the pinhole was set to give an optical slice of ~2 μm. The FAD redox index and mitochondrial pool were estimated by sequentially applying 1 μM of the mitochondrial uncoupler FCCP (carbonyl cyanide p-trifluoromethoxyphenylhydrazone), followed by 1 mM of the complex IV inhibitor sodium cyanide. Application of FCCP maximizes respiration and completely oxidizes the mitochondrial pool of $FADH_2$, manifesting as an increase in FAD fluorescence. Conversely, sodium cyanide suppresses respiration, preventing $FADH_2$ oxidation and allowing the $FADH_2$ pool to regenerate fully, manifesting as a decrease in FAD fluorescence. The redox index is expressed as a percentage of basal FAD autofluorescence compared with the maximal (in response to FCCP) and the minimal (in response to sodium cyanide) fluorescence, whereas the difference between these values represents the total mitochondrial pool of FAD [32]. The NADH mitochondrial pool and redox index were determined in an

analogous manner. The NADH autofluorescence was measured with excitation at 405 nm and emission at 440–480 nm. To determine the ATP levels in mitAT1.03-transfected cells, FRET was quantified by the 527:475 nm ratio using excitation at 405 nm and a filter from 515 to 580 nm [12,31]. Acute slices (three for each genotype) and cultured cells were imaged in glucose-free HBSS (Hanks balanced salt solution) [1.26 mM $CaCl_2$, 0.493 mM $MgCl_2$, 0.407 mM $MgSO_4$, 5.33 mM KCl, 0.441 mM KH_2PO_4, 4.17 mM $NaHCO_3$, 137.93 mM NaCl and 0.338 mM Na_2HPO_4 (pH 7.4)]. Data were generated from a minimum of three independent experiments (acute heart slices or coverslips with plated MEFs, using the value of mean attenuance for each preparation).

Oxygen consumption

Cells ($\sim2\times10^6$) were suspended in glucose-free HBSS in a Clark-type oxygen electrode (Hansatech) thermostatically maintained at 37°C, which was calibrated with air-saturated water, assuming 406 ng of oxygen atoms/ml at 37°C. Oxygen consumption was measured with the addition of palmitic acid (0.4 mM), oligomycin (2 μg/ml) and FCCP. The concentration of FCCP, which induces maximal respiration, was determined on the day of each experiment. For the cells used in the present study, the maximal rate of oxygen consumption was induced by 1 μM FCCP. To determine the respiratory control ratio, intact mitochondria were isolated from the brain, liver and heart of female WT, Keap1-KD and Nrf2-KO mice by differential centrifugation [33]. Mitochondria were then resuspended in respiration medium [135 mM KCl, 10 mM NaCl, 20 mM Hepes, 0.5 mM KH_2PO_4, 1 mM $MgCl_2$ and 5 mM EGTA (pH 7.1)], also containing 1.86 mM $CaCl_2$ to yield a free [Ca^{2+}] of ~100 nM, and oxygen consumption was measured in a Clark-type oxygen electrode thermostatically maintained at 25°C. Palmitic acid (0.4 mM), palmitoylcarnitine (0.1 mM) and glutamate (5 mM) were added sequentially. Data were obtained using an Oxygraph Plus system with Chart recording software.

Quantitative real-time PCR

The primers and probes used to quantify the levels of mRNA for SCAD (short-chain acyl-CoA dehydrogenase) (*Acads*), MCAD (medium-chain acyl-CoA dehydrogenase) (*Acadm*), LCAD (long-chain acyl-CoA dehydrogenase) (*Acadl*) and VLCAD (very-long-chain acyl-CoA dehydrogenase) (*Acadvl*) were obtained from Applied Biosystems (assay IDs: Mm00431617_m1, Mm01323360_g1, Mm00599660_m1 and Mm00444293_m1 respectively). Total RNA was extracted from the liver tissue of female WT, Nrf2-KO and Keap1-KD C57BL/6 mice using RNeasy Kit (Qiagen). Total RNA (500 ng) was reverse transcribed into cDNA with Omniscript Reverse Transcription Kit (Qiagen). Real-time PCR was performed in triplicates on Applied Biosystems 7900HT Fast Real-Time PCR System. The TaqMan® data for the mRNA species were normalized using β-actin (mouse ACTB, Applied Biosystems, Mm00607939_s1) as an internal control.

Statistical analysis

Statistical analysis was performed using the Origin 9.0 software (Microcal Software). Statistical significance for multiple comparisons was performed by Student's *t* test. In all cases, a confidence interval of 95% or $P < 0.05$ was considered to be statistically significant.

RESULTS AND DISCUSSION

Nrf2 alters the efficiency of mitochondrial oxidation of palmitic acid

To test whether the status of Nrf2 activity affects the efficiency of mitochondrial FAO, we first used MEFs isolated from WT, Nrf2-KO and Keap1-KO mice. Compared with WT cells, the levels of Nrf2 are higher in Keap1-KO and undetectable in Nrf2-KO MEFs (Figure 1A). This correlates well with the enzyme activity of the prototypic Nrf2-dependent enzyme NQO1 which, in comparison with WT MEFs, is 10-fold higher in their Keap1-KO and 10-fold lower in their Nrf2-KO counterparts (Figure 1B).

We first evaluated the rate of oxygen consumption after the addition of palmitic acid (0.4 mM). Oxygen consumption was linear over the period of measurement (Figure 1C). Importantly, at the same concentration, application of this long-chain ($C_{16:0}$) fatty acid produced a significantly higher (1.24-fold) rate of respiration in Keap1-KO MEFs ($n = 4$; $P < 0.01$), whereas in Nrf2-deficient cells, the rate of respiration was significantly lower (36%) when compared with WT ($n = 4$; $P < 0.01$) (Figure 1D). These differences among the genotypes suggest that the efficiency of FAO is influenced by the status of Nrf2, whereby FAO is impaired in the absence of the transcription factor and accelerated under conditions of constitutive Nrf2 activation.

Inhibition of the F_1F_o-ATP synthase by oligomycin (2 μg/ml) suppresses respiration coupled to oxidative phosphorylation. This inhibitor decreased respiration to a similar rate (0.38 ng of oxygen/min per 10^6 cells) in all genotypes (Figure 1D, oligomycin). However, compared with WT, the difference in respiratory rate in the absence (basal rate of ATP synthesis) and in the presence (no ATP production) of oligomycin was significantly bigger (1.4-fold; $n = 4$; $P < 0.01$) in Keap1-KO and smaller (33%; $n = 4$; $P < 0.01$) in Nrf2-KO MEFs, suggesting that, following oxidation of palmitic acid, the Nrf2 activity affects respiration and oxidative phosphorylation.

Application of the uncoupler FCCP induces maximal respiration of mitochondria. In this experimental system, addition of FCCP (1 μM) caused a significantly higher respiration in Keap1-KO ($n = 4$; $P < 0.01$) and significantly lower respiration in Nrf2-KO MEFs ($n = 4$; $P < 0.01$) (Figure 1D, FCCP) when compared with WT cells. We have reported previously that the *in vitro* enzyme activities of the respiratory chain complexes are not affected by the Nrf2 status [12]. Taken together, these results suggest that the altered maximal respiration under conditions of Nrf2 deficiency or constitutive activation may be due to differences in substrate availability following oxidation of palmitic acid.

Nrf2 affects the production of ATP following mitochondrial oxidation of palmitic acid

Mitochondrial FAO represents an important source for ATP production in different tissues, especially under conditions of glucose deprivation. Its end product, acetyl-CoA, enters the TCA (tricarboxylic acid) cycle, which then generates NADH and $FADH_2$. In addition, mitochondrial FAO also can affect mitochondrial respiration and ATP production by directly transferring electrons to ubiquinone through the activities of acyl-CoA dehydrogenases. Therefore we next investigated whether, in the absence of glucose, addition of palmitic acid differentially affects the production of ATP in MEFs of the three genotypes.

This part of the present study employed a genetically encoded FRET-based indicator for ATP [31]. We found that application of palmitic acid induced a small increase in ATP levels in WT cells (Figure 2A). As expected, subsequent application of oligomycin (2 μg/ml) led to a decrease in ATP levels. In contrast, application of palmitic acid to Keap1-KO or Nrf2-KO MEF cells did not cause any detectable increase in the ATP levels (Figures 2B and 2C). Interestingly, compared with WT, the ATP levels were more strongly affected by oligomycin in Keap1-KO cells (1.3-fold; $n = 8$; $P < 0.01$), whereas only a small decrease was recorded in Nrf2-deficient MEFs (40% of WT; $n = 3$; $P < 0.01$) (Figure 2D). These results are in close agreement with our previous observations in primary cortical neurons where either Nrf2 deficiency or its constitutive up-regulation decreases the contribution of oxidative phosphorylation to ATP production in favour of glycolysis [12].

The initial step in mitochondrial FAO is the α-β dehydrogenation of the acyl-CoA fatty acid ester. As the α-carbon is being deprotonated, the pro-R hydrogen of the β-carbon leaves as a hydride, reducing the FAD cofactor to FADH$_2$. FADH$_2$ then transfers electrons to ubiquinone in the respiratory chain via the electron transfer flavoprotein ubiqionone oxidoreductase [34]. To determine whether this process could be responsible for the Nrf2-dependent alterations in ATP levels that we observed in the mutant cells, we inhibited mitochondrial complexes I and II by using rotenone (5 μM) and malonate (20 μM). This was then followed by stimulation with the carnitine conjugate of palmitic acid, palmitoylcarnitine (0.1 mM). Stimulation of FAO induced an increase in the mitochondrial ATP levels in both WT (25%, $n = 4$) and to a higher degree in Keap1-KO (35%, $n = 4$) cells (Figures 3A and 3B). In sharp contrast, application of palmitoylcarnitine did not change the mitochondrial ATP levels in Nrf2-KO MEFs (n 4) (Figure 3A). This result confirms that, in the absence of= Nrf2, FAO is suppressed. Moreover, it indicates that the lower ATP levels in the Nrf2-deficient cells are, at least in part, due to suppression of FAO.

Nrf2 is a master regulator of the cellular redox homoeostasis. It was therefore possible that the observed suppression of FAO under conditions of Nrf2 deficiency is due to the decrease in the antioxidant defences and the accumulation of ROS in the Nrf2-KO cells [11,12]. Indeed, a number of mitochondrial proteins, including enzymes involved in FAO, contain redox-sensitive cysteine residues, the oxidation of which affects the enzyme activity [35]. Pre-treatment with the antioxidant trolox (6 h, 100 μM), a water-soluble analogue of vitamin E, had no effect on the lack of response of Nrf2-KO MEFs to stimulation with palmitoylcarnitine in the presence of inhibitors of complexes I and II ($n = 4$) (Figure 3C), suggesting that the effect of Nrf2 on FAO-induced ATP production is largely independent of the antioxidant role of the transcription factor.

Nrf2 alters mitochondrial respiration following stimulation of FAO

To investigate further the consequences of Nrf2-mediated alterations in FAO on mitochondrial metabolism, we isolated mitochondria from mice in which Nrf2 is either genetically deleted or constitutively activated, and compared them with their WT counterparts. As Keap1-KO mice die postnatally from starvation caused by oesophageal hyperkeratosis [27], in the subsequent experiments we used Keap1-KD mice. These animals carry the floxed allele of the *keap1* gene (*keap1*$^{\text{flox/flox}}$), resulting in its reduced expression

and, consequently, Nrf2 accumulation and increased expression of Nrf2-target genes [26]. The rate of oxygen consumption was measured in mitochondria isolated from the brain, liver and heart of animals of the three genotypes. Palmitic acid (0.4 mM) did not activate the rate of respiration in WT brain mitochondria (Figure 4A), in agreement with previously published data [36]. Similar to the free fatty acid, application of its carnitine conjugate, palmitoylcarnitine (50 μM), did not aid brain mitochondrial respiration. In contrast, glutamate (5 mM) strongly stimulated respiration, demonstrating that the brain mitochondria were healthy, but unresponsive to palmitic acid stimulation.

In contrast with the findings with brain mitochondria, addition of palmitic acid to WT liver and heart mitochondria strongly stimulated State 2 respiration (Figures 4B and 4C). The rate of oxygen consumption of the liver preparations from WT animals was 145 ± 10.8 ng of atom oxygen/min per mg of protein ($n = 5$) (Figure 4D). Interestingly, the effect of palmitic acid in Nrf2-KO liver mitochondria was significantly weaker, by ~30% (102 ± 8.4; $n = 3$; $P < 0.01$), whereas a significantly higher (1.4-fold) respiration was detected in liver mitochondria of Keap1-KD mice (206 ± 19; $n = 3$; $P < 0.01$). A very similar observation was recorded in mitochondria isolated from heart of WT, Nrf2-KO and Keap1-KD mice (work not shown). Importantly, the decrease in Nrf2-KO and the activation in Keap1-KD mitochondria in comparison with their WT counterparts is not due to defects in the carnitine shuttle as application of palmitoylcarnitine did not reverse the State 2 respiration back to WT levels, and the differences among the genotypes remained unchanged (Figure 4D). Furthermore, the activation of the mitochondrial respiration with palmitic acid or palmitoylcarnitine was not associated with uncoupling of the respiratory chain as the ratio of State 3/State 4 respiration was higher in WT and Keap1-KD mitochondria, but lower in their Nrf2-KO counterparts (Figure 4E).

The similarities of the responses to palmitic acid and its carnitine conjugate palmitoylcarnitine, indicated that the underlying reasons for the differences among the genotypes are unlikely to be due to altered function of CPT1, the enzyme which mediates the transport of long-chain fatty acids across the mitochondrial membrane by binding them to carnitine [37]. To test further this conclusion, we used the short chain ($C_{6:0}$) fatty acid, hexanoic acid, which is not a substrate for CPT1 [38]. Application of hexanoic acid (0.5 mM) mirrored the State 2 respiration results obtained after application of palmitic acid (Figure 4F), confirming that the respiratory defect of the mitochondria from the mutant mice is independent of CPT1.

Nrf2 affects the rates of FADH$_2$ generation and utilization

We demonstrated recently that following inhibition of complex IV with sodium cyanide, the rates of regeneration of FADH$_2$ are much lower in Nrf2-KO primary cortical neurons compared with cells that are either WT for the transcription factor or have constitutively active Nrf2 [12]. As each cycle of FAO generates FADH$_2$, which then enters the respiratory chain, we next investigated the rate of FADH$_2$ production following application of hexanoic acid to acute heart slices by monitoring the FAD autofluorescence in a live-cell imaging experiment. In WT slices, application of hexanoic acid (0.5 mM) induced a transient increase in FAD levels, suggesting an activation of complex II respiration (Figure 5A). This

transient increase was followed by a recovery back to basal levels. As expected, further application of FCCP (1 μM) to the acute heart slice maximized the FAD levels, whereas sodium cyanide (1 mM) minimized them (Figure 5A).

In comparison with WT, the application of FCCP and sodium cyanide resulted in greater responses in Keap1-deficient slices (Figure 5B). In sharp contrast, in Nrf2-KO heart slices, hexanoic acid induced only a small increase in FAD levels (Figure 5C). Furthermore, FCCP did not have any effect on the levels of FAD, strongly suggesting that Nrf2-KO mitochondria were already respiring at their maximal capacity. Compared with WT and Keap1-KD slices, the rate of recovery of the FAD pool after addition of sodium cyanide was lower in Nrf2-KO slices (Figure 5D). Parallel experiments with palmitic acid in heart slices, and with both the short-chain (hexanoic) and long-chain (palmitic) fatty acids in acute liver slices gave identical results (not shown). Taken together, these findings implicate the influence of Nrf2 on FAO as one potential mechanism responsible for the altered respiration and ATP production under conditions of Nrf2 deficiency or constitutive up-regulation.

As mentioned above, $FADH_2$ is produced at each cycle of FAO during the α-β dehydrogenation of the acyl-CoA fatty acid ester. This reaction is catalysed by the acyl-CoA dehydrogenases, a family of four chain-length-specific enzymes, comprising VLCADs, LCADs, MCADs and SCADs. It was therefore possible that the differences in the rate of $FADH_2$ production among the genotypes upon application of fatty acids were due to differences in the gene expression for some of these enzymes. To test this possibility, we determined the hepatic mRNA levels for SCAD, MCAD, LCAD and VLCAD. Quantitative real-time PCR (TaqMan®) analysis showed that the mRNA levels for SCAD, LCAD and VLCAD were not significantly different among the three genotypes (Figure 6). The only exception was MCAD, the expression of which showed a small ~25% decrease in the Nrf2-KO in comparison with WT. These similarities in the pattern of gene expression are unlikely to explain the phenotypic differences in respiration and ATP production among the genotypes.

In human tissues, 80% of the palmitoyl-CoA dehydrogenation activity is due to VLCAD [39]. Importantly, VLCAD is one of the proteins which contain cysteine residues that significantly change their redox state following exposure of isolated rat heart mitochondria to H_2O_2 as well as following endogenous H_2O_2 generation [35]. It was therefore possible that the enzyme activity of VLCAD was lower in the Nrf2-KO MEFs due to the higher levels of ROS in these cells, ultimately lowering the $FADH_2$ production. In order to investigate whether the Nrf2-mediated changes in the antioxidant levels are responsible for the observed differences among the genotypes with respect to the rates of $FADH_2$ generation and utilization, we incubated WT, Keap1- and Nrf2-deficient MEFs with 100 μM trolox for 6 h. Pre-incubation of the WT cells with the antioxidant significantly increased the mitochondrial NADH pool and reduced the mitochondrial FAD pool ($n = 36$) (Figures 7A and 7B); estimated as the difference between the maximal (in response to FCCP) and the minimal (in response to sodium cyanide) values. Incubation with the antioxidant in Nrf2-KO cells also increased the NADH pool significantly, but did not affect the FAD pool ($n = 41$). The antioxidant had no effect on either the NADH or the FAD pools in Keap1-KO cells ($n = 33$). Despite the significant increase in the NADH pool in WT and Nrf2-KO cells in

response to incubation with trolox, the mitochondrial redox index of WT, Keap1-KO and Nrf2-KO MEFs, reflecting the balance between NADH (or FAD) production and consumption, remained unchanged (Figures 7C and 7D). This result indicates that the increase in the NADH pool is still not sufficient to normalize the defects in respiration and ATP production.

In conclusion, in the present study, we provide functional evidence in isolated mitochondria, cells and acute tissue slices that the activity of Nrf2 has a significant impact on the efficiency of FAO, ultimately affecting mitochondrial metabolism and bioenergetics. Although the underlying reason for this is not understood at present, the effect of Nrf2 on FAO strongly suggests that, by altering mitochondrial metabolism, the activity of this transcription factor may profoundly influence health and disease. The results presented in the present study are consistent with two recent human metabolomic profiling studies showing changes in acylcarnitine and FAD levels in plasma and urine following intervention with diets rich in glucosinolates (precursors of the Nrf2-inducing isothiocyanates), indicative of enhanced integration of FAO with the activity of the TCA cycle [40,41]. Our findings provide new knowledge of the versatile Nrf2-regulated networks which extend beyond the stress response to electrophiles and oxidants to include most basic cellular processes such as FAO, the disturbances of which have broad implications for the pathogenesis of numerous pathological processes, such as cancer, metabolic syndrome and neurodegenerative conditions.

Acknowledgments

Abbreviations

CPT1	carnitine palmitoyltransferase 1
FAO	fatty acid oxidation
FAS	fatty acid synthesis
FCCP	carbonyl cyanide *p*-trifluoromethoxyphenylhydrazone
G6PD	glucose-6-phosphate dehydrogenase
HBSS	Hanks balanced salt solution
KD	knockdown
Keap1	Kelch-like ECH-associated protein 1
KO	knockout

LCAD	long-chain acyl-CoA dehydrogenase
MCAD	medium-chain acyl-CoA dehydrogenase
MEF	mouse embryonic fibroblast
NQO1	NAD(P)H:quinone oxidoreductase 1
Nrf2	NF-E2 p45-related factor 2
ROS	reactive oxygen species
SCAD	short-chain acyl-CoA dehydrogenase
TCA	tricarboxylic acid
VLCAD	very-long-chain acyl-CoA dehydrogenase
WT	wild-type

REFERENCES

1. Talalay P. Chemoprotection against cancer by induction of phase 2 enzymes. Biofactors. 2000; 12:5–11. [PubMed: 11216505]

2. Hayes JD, McMahon M, Chowdhry S, Dinkova-Kostova AT. Cancer chemoprevention mechanisms mediated through the Keap1-Nrf2 pathway. Antioxid. Redox Signal. 2010; 13:1713–1748. [PubMed: 20446772]

3. Kensler TW, Wakabayashi N, Biswal S. Cell survival responses to environmental stresses via the Keap1-Nrf2-ARE pathway. Annu. Rev. Pharmacol. Toxicol. 2007; 47:89–116. [PubMed: 16968214]

4. Kobayashi M, Yamamoto M. Nrf2-Keap1 regulation of cellular defense mechanisms against electrophiles and reactive oxygen species. Adv. Enzyme Regul. 2006; 46:113–140. [PubMed: 16887173]

5. Villeneuve NF, Lau A, Zhang DD. Regulation of the Nrf2-Keap1 antioxidant response by the ubiquitin proteasome system: an insight into cullin-ring ubiquitin ligases. Antioxid. Redox Signal. 2010; 13:1699–1712. [PubMed: 20486766]

6. Wild AC, Moinova HR, Mulcahy RT. Regulation of γ-glutamylcysteine synthetase subunit gene expression by the transcription factor Nrf2. J. Biol. Chem. 1999; 274:33627–33636. [PubMed: 10559251]

7. Thimmulappa RK, Mai KH, Srisuma S, Kensler TW, Yamamoto M, Biswal S. Identification of Nrf2-regulated genes induced by the chemopreventive agent sulforaphane by oligonucleotide microarray. Cancer Res. 2002; 62:5196–5203. [PubMed: 12234984]

8. Lee JM, Calkins MJ, Chan K, Kan YW, Johnson JA. Identification of the NF-E2-related factor-2-dependent genes conferring protection against oxidative stress in primary cortical astrocytes using oligonucleotide microarray analysis. J. Biol. Chem. 2003; 278:12029–12038. [PubMed: 12556532]

9. Wu KC, Cui JY, Klaassen CD. Beneficial role of nrf2 in regulating NADPH generation and consumption. Toxicol. Sci. 2011; 123:590–600. [PubMed: 21775727]

10. Mitsuishi Y, Taguchi K, Kawatani Y, Shibata T, Nukiwa T, Aburatani H, Yamamoto M, Motohashi H. Nrf2 redirects glucose and glutamine into anabolic pathways in metabolic reprogramming. Cancer Cell. 2012; 22:66–79. [PubMed: 22789539]

11. Wakabayashi N, Dinkova-Kostova AT, Holtzclaw WD, Kang MI, Kobayashi A, Yamamoto M, Kensler TW, Talalay P. Protection against electrophile and oxidant stress by induction of the phase 2 response: fate of cysteines of the Keap1 sensor modified by inducers. Proc. Natl. Acad. Sci. U.S.A. 2004; 101:2040–2045. [PubMed: 14764894]

12. Holmstrom KM, Baird L, Zhang Y, Hargreaves I, Chalasani A, Land JM, Stanyer L, Yamamoto M, Dinkova-Kostova AT, Abramov AY. Nrf2 impacts cellular bioenergetics by controlling

substrate availability for mitochondrial respiration. Biol. Open. 2013; 2:761–770. [PubMed: 23951401]

13. Benedict AL, Knatko EV, Dinkova-Kostova AT. The indirect antioxidant sulforaphane protects against thiopurine-mediated photooxidative stress. Carcinogenesis. 2012; 33:2457–2466. [PubMed: 22983983]

14. Schafer ZT, Grassian AR, Song L, Jiang Z, Gerhart-Hines Z, Irie HY, Gao S, Puigserver P, Brugge JS. Antioxidant and oncogene rescue of metabolic defects caused by loss of matrix attachment. Nature. 2009; 461:109–113. [PubMed: 19693011]

15. Nguyen D, Samson SL, Reddy VT, Gonzalez EV, Sekhar RV. Impaired mitochondrial fatty acid oxidation and insulin resistance in aging: novel protective role of glutathione. Aging Cell. 2013; 12:415–425. [PubMed: 23534396]

16. Yates MS, Tran QT, Dolan PM, Osburn WO, Shin S, McCulloch CC, Silkworth JB, Taguchi K, Yamamoto M, Williams CR, et al. Genetic versus chemoprotective activation of Nrf2 signaling: overlapping yet distinct gene expression profiles between Keap1 knockout and triterpenoid-treated mice. Carcinogenesis. 2009; 30:1024–1031. [PubMed: 19386581]

17. Chowdhry S, Nazmy MH, Meakin PJ, Dinkova-Kostova AT, Walsh SV, Tsujita T, Dillon JF, Ashford ML, Hayes JD. Loss of Nrf2 markedly exacerbates nonalcoholic steatohepatitis. Free Radic. Biol. Med. 2010; 48:357–371. [PubMed: 19914374]

18. Sugimoto H, Okada K, Shoda J, Warabi E, Ishige K, Ueda T, Taguchi K, Yanagawa T, Nakahara A, Hyodo I, et al. Deletion of nuclear factor-E2-related factor-2 leads to rapid onset and progression of nutritional steatohepatitis in mice. Am. J. Physiol. Gastroinstest. Liver Physiol. 2010; 298:G283–G294. [PubMed: 19926817]

19. Kitteringham NR, Abdullah A, Walsh J, Randle L, Jenkins RE, Sison R, Goldring CE, Powell H, Sanderson C, Williams S, et al. Proteomic analysis of Nrf2 deficient transgenic mice reveals cellular defence and lipid metabolism as primary Nrf2-dependent pathways in the liver. J. Proteomics. 2010; 73:1612–1631. [PubMed: 20399915]

20. Flowers MT, Ntambi JM. Role of stearoyl-coenzyme A desaturase in regulating lipid metabolism. Curr. Opin. Lipidol. 2008; 19:248–256. [PubMed: 18460915]

21. Tanaka Y, Ikeda T, Yamamoto K, Ogawa H, Kamisako T. Dysregulated expression of fatty acid oxidation enzymes and iron-regulatory genes in livers of Nrf2-null mice. J. Gastroenterol. Hepatol. 2012; 27:1711–1717. [PubMed: 22591204]

22. Mannaerts GP, Debeer LJ. Mitochondrial and peroxisomal β-oxidation of fatty acids in rat liver. Ann. N.Y. Acad. Sci. 1982; 386:30–39. [PubMed: 6953849]

23. Carracedo A, Cantley LC, Pandolfi PP. Cancer metabolism: fatty acid oxidation in the limelight. Nat. Rev. Cancer. 2013; 13:227–232. [PubMed: 23446547]

24. Itoh K, Chiba T, Takahashi S, Ishii T, Igarashi K, Katoh Y, Oyake T, Hayashi N, Satoh K, Hatayama I, et al. An Nrf2/small Maf heterodimer mediates the induction of phase II detoxifying enzyme genes through antioxidant response elements. Biochem. Biophys. Res. Commun. 1997; 236:313–322. [PubMed: 9240432]

25. Chanas SA, Jiang Q, McMahon M, McWalter GK, McLellan LI, Elcombe CR, Henderson CJ, Wolf CR, Moffat GJ, Itoh K, et al. Loss of the Nrf2 transcription factor causes a marked reduction in constitutive and inducible expression of the glutathione S-transferase Gsta1, Gsta2, Gstm1, Gstm2, Gstm3 and Gstm4 genes in the livers of male and female mice. Biochem. J. 2002; 365:405–416. [PubMed: 11991805]

26. Taguchi K, Maher JM, Suzuki T, Kawatani Y, Motohashi H, Yamamoto M. Genetic analysis of cytoprotective functions supported by graded expression of Keap1. Mol. Cell. Biol. 2010; 30:3016–3026. [PubMed: 20404090]

27. Wakabayashi N, Itoh K, Wakabayashi J, Motohashi H, Noda S, Takahashi S, Imakado S, Kotsuji T, Otsuka F, Roop DR, et al. Keap1-null mutation leads to postnatal lethality due to constitutive Nrf2 activation. Nat. Genet. 2003; 35:238–245. [PubMed: 14517554]

28. Higgins LG, Hayes JD. The cap'n'collar transcription factor Nrf2 mediates both intrinsic resistance to environmental stressors and an adaptive response elicited by chemopreventive agents that determines susceptibility to electrophilic xenobiotics. Chem. Biol. Interact. 2011; 192:37–45. [PubMed: 20932822]

29. McMahon M, Itoh K, Yamamoto M, Hayes JD. Keap1-dependent proteasomal degradation of transcription factor Nrf2 contributes to the negative regulation of antioxidant response element-driven gene expression. J. Biol. Chem. 2003; 278:21592–21600. [PubMed: 12682069]

30. Fahey JW, Dinkova-Kostova AT, Stephenson KK, Talalay P. The "Prochaska" microtiter plate bioassay for inducers of NQO1. Methods Enzymol. 2004; 382:243–258. [PubMed: 15047106]

31. Imamura H, Nhat KP, Togawa H, Saito K, Iino R, Kato-Yamada Y, Nagai T, Noji H. Visualization of ATP levels inside single living cells with fluorescence resonance energy transfer-based genetically encoded indicators. Proc. Natl. Acad. Sci. U.S.A. 2009; 106:15651–15656. [PubMed: 19720993]

32. Gandhi S, Wood-Kaczmar A, Yao Z, Plun-Favreau H, Deas E, Klupsch K, Downward J, Latchman DS, Tabrizi SJ, Wood NW, et al. PINK1-associated Parkinson's disease is caused by neuronal vulnerability to calcium-induced cell death. Mol. Cell. 2009; 33:627–638. [PubMed: 19285945]

33. Domijan AM, Abramov AY. Fumonisin B1 inhibits mitochondrial respiration and deregulates calcium homeostasis-implication to mechanism of cell toxicity. Int. J. Biochem. Cell Biol. 2011; 43:897–904. [PubMed: 21397036]

34. Watmough NJ, Frerman FE. The electron transfer flavoprotein: ubiquinone oxidoreductases. Biochim. Biophys. Acta. 2010; 1797:1910–1916. [PubMed: 20937244]

35. Hurd TR, Prime TA, Harbour ME, Lilley KS, Murphy MP. Detection of reactive oxygen species-sensitive thiol proteins by redox difference gel electrophoresis: implications for mitochondrial redox signaling. J. Biol. Chem. 2007; 282:22040–22051. [PubMed: 17525152]

36. Ronnett GV, Kleman AM, Kim EK, Landree LE, Tu Y. Fatty acid metabolism, the central nervous system, and feeding. Obesity. 2006; 14:201S–207S. [PubMed: 17021367]

37. Abumrad NA, Perkins RC, Park JH, Park CR. Mechanism of long chain fatty acid permeation in the isolated adipocyte. J. Biol. Chem. 1981; 256:9183–9191. [PubMed: 7263707]

38. Abumrad NA, Park JH, Park CR. Permeation of long-chain fatty acid into adipocytes. Kinetics, specificity, and evidence for involvement of a membrane protein. J. Biol. Chem. 1984; 259:8945–8953. [PubMed: 6746632]

39. Aoyama T, Souri M, Ushikubo S, Kamijo T, Yamaguchi S, Kelley RI, Rhead WJ, Uetake K, Tanaka K, Hashimoto T. Purification of human very-long-chain acyl-coenzyme A dehydrogenase and characterization of its deficiency in seven patients. J. Clin. Invest. 1995; 95:2465–2473. [PubMed: 7769092]

40. Armah CN, Traka MH, Dainty JR, Defernez M, Janssens A, Leung W, Doleman JF, Potter JF, Mithen RF. A diet rich in high-glucoraphanin broccoli interacts with genotype to reduce discordance in plasma metabolite profiles by modulating mitochondrial function. Am. J. Clin. Nutr. 2013; 98:712–722. [PubMed: 23964055]

41. May DH, Navarro SL, Ruczinski I, Hogan J, Ogata Y, Schwarz Y, Levy L, Holzman T, McIntosh MW, Lampe JW. Metabolomic profiling of urine: response to a randomised, controlled feeding study of select fruits and vegetables, and application to an observational study. Br. J. Nutr. 2013; 110:1760–1770. [PubMed: 23657156]
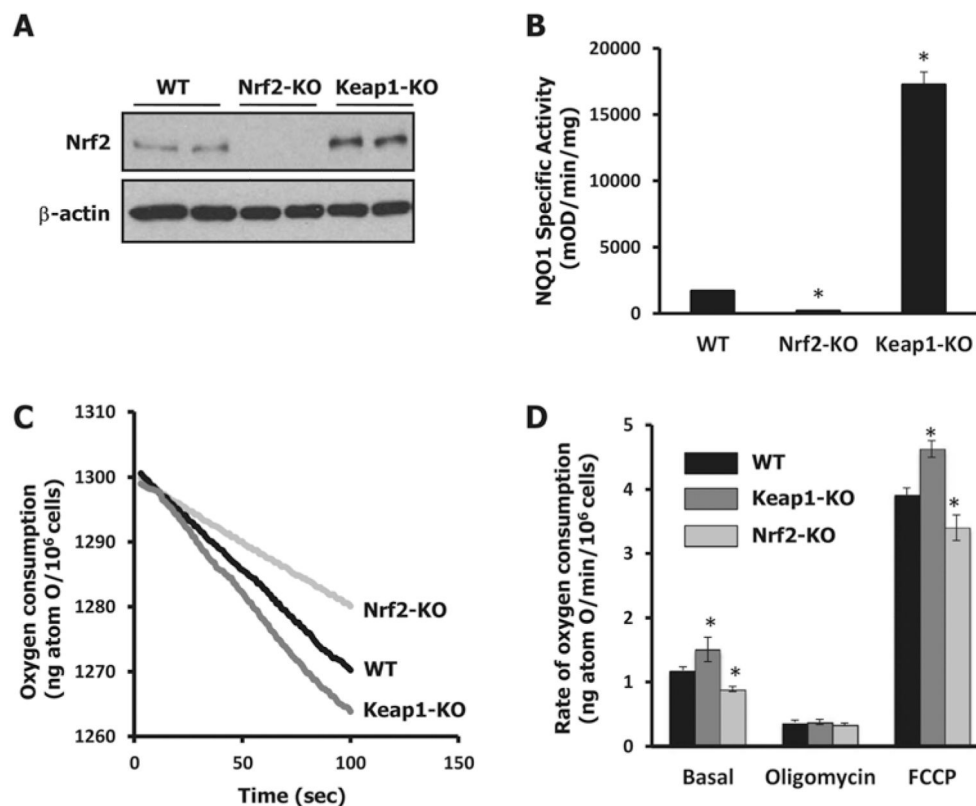
Figure 1. Nrf2 alters the efficiency of mitochondrial oxidation of palmitic acid

(**A**) Compared with WT cells, the levels of Nrf2 are higher in Keap1-KO, and undetectable in Nrf2-KO MEFs. (**B**) The enzyme activity of the Nrf2-target protein NQO1 is 10-fold lower in Nrf2-KO and 10-fold higher in Keap1-KO MEFs in comparison with WT cells. (**C**) Oxygen consumption was measured in aliquots of WT, Nrf2-KO and Keap1-KO MEF cell suspensions ($\sim2\times10^6$) in glucose-free HBSS in the presence of palmitic acid (0.4 mM). Compared with WT, oxygen consumption was higher in Keap1-KO cells and lower in Nrf2-deficient cells. (**D**) Oxygen consumption rate in cell suspensions of WT (black bars), Keap1-KO (dark grey bars) and Nrf2-KO (light grey bars) MEFs in HBSS in the presence of palmitic acid (0.4 mM) and the absence of glucose. The contribution of oxidative phosphorylation was estimated through application of oligomycin (F_1F_o-ATP synthase inhibitor; 2 μg/ml). The maximal rate of respiration was estimated after addition of FCCP (1 μM). Data are presented as means $\pm$ S.E.M. *$P<0.01$ compared with WT.
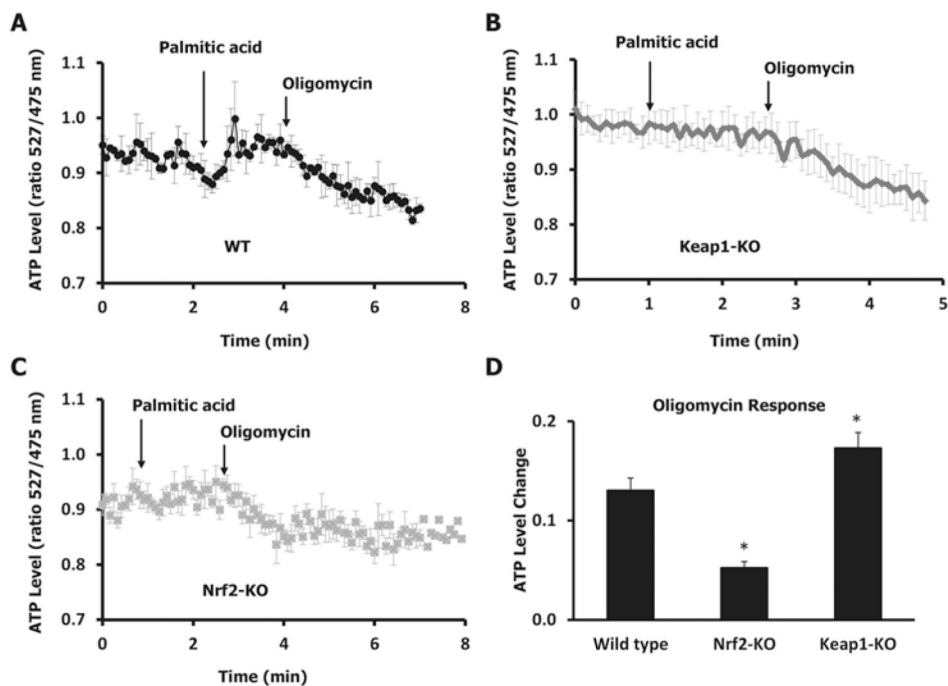
Figure 2. Nrf2 affects the production of ATP following mitochondrial oxidation of palmitic acid
Live-cell measurements of the ATP levels in WT (**A**), Keap1-KO (**B**) and Nrf2-KO (**C**)
MEFs show differences among the genotypes in response to palmitic acid (0.4 mM) and
oligomycin (2 μg/ml). (**D**) Quantification of the decrease in the ATP levels in response to
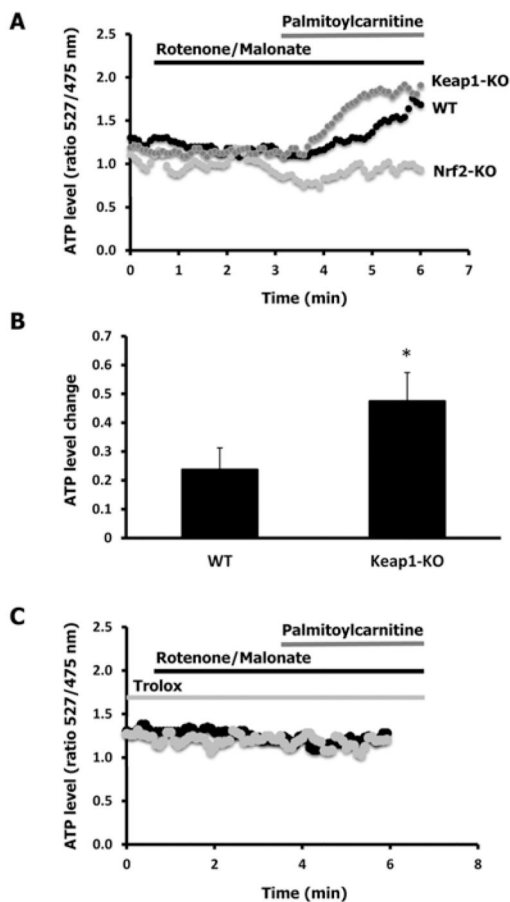oligomycin. Data are presented as means ± S.E.M. *$P < 0.01$ compared with WT.

Figure 3. Nrf2 affects the production of ATP following mitochondrial oxidation of palmitoylcarnitine acid in the presence of inhibitors of complexes I and II

(**A**) Live–cell measurements of the mitochondrial ATP levels in WT, Keap1-KO and Nrf2-KO MEFs show differences among the genotypes in response to palmitoylcarnitine (0.1 mM) in the presence of rotenone (5 μM) and malonate (20 μM). (**B**) Quantification of the increase in the ATP levels in response to palmitoylcarnitine in WT and Keap1-KO MEFs. (**C**) Live-cell measurements of the ATP levels in response to palmitoylcarnitine (0.1 mM) in the presence of rotenone (5 μM) and malonate (20 μM) in Nrf2-KO MEFs which had been pre-treated for 6 h with the antioxidant trolox. Two representative traces are shown. Data are presented as means $\pm$ S.E.M. *P<0.01.
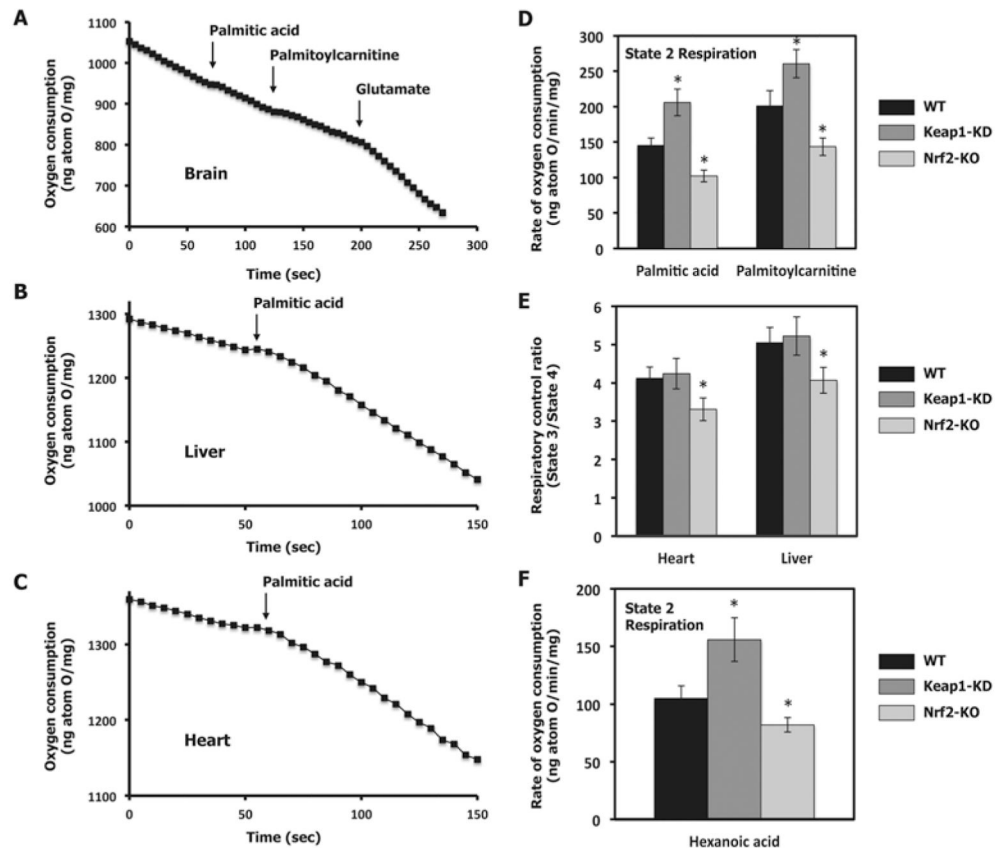
Figure 4. Nrf2 alters mitochondrial respiration upon stimulation of FAO

(**A**) Isolated mitochondria from the brain did not show any acceleration of oxygen consumption in response to palmitic acid or its conjugate. Activation of respiration through application of glutamate demonstrated that these mitochondria were intact. Oxygen consumption in WT brain mitochondria was monitored at basal state, and after the sequential addition of palmitic acid (0.4 mM), palmitoylcarnitine (50 μM) and glutamate (5 mM). (**B** and **C**) Oxygen consumption was strongly accelerated in mitochondria from the liver (**B**) and heart (**C**) following the addition of palmitic acid (0.4 mM). (**D**) State 2 respiration (respiration with substrates, but before application of ADP) in isolated liver mitochondria from WT (black bars), Keap1-KD (dark grey bars) and Nrf2-KO (light grey bars) mice in the presence of palmitic acid (0.4 mM) or palmitoylcarnitine (50 μM). The value of State 2 respiration is highest in Keap1-KD and lowest in Nrf2-KO when compared with WT liver mitochondria. (**E**) Respiratory control ratio, State 3 respiration [ADP (substrate for ATP synthesis)-dependent] to State 4 respiration (ADP-independent, ADP consumed by mitochondria), in isolated mitochondria from the heart and liver of WT (black bars), Keap1-KD (dark grey bars) and Nrf2-KO (light grey bars) mice. (**F**) State 2 respiration in isolated liver mitochondria from WT (black bars), Keap1-KD (dark grey bars) and Nrf2-KO (light grey bars) mice in the presence of hexanoic acid (0.5 mM). The effect of hexanoic acid mirrored the results obtained with palmitic acid. Data are presented as means ± S.E.M. *$P < 0.01$ compared with WT.
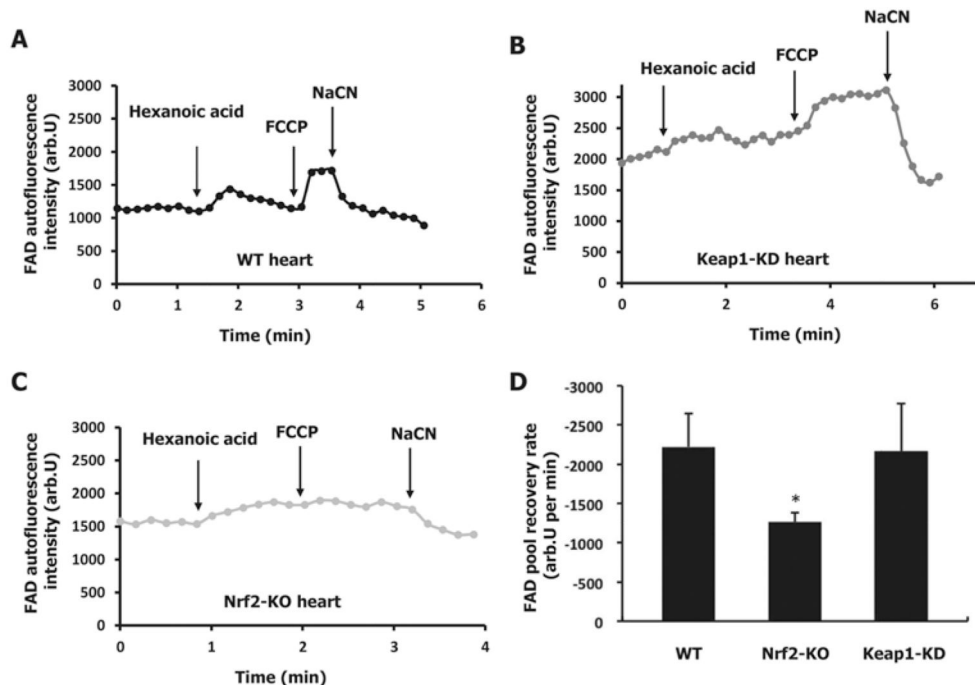
Figure 5. Nrf2 affects the rates of FADH$_2$ generation and utilization
FAD levels were determined in acute heart slices prepared from WT (**A**), Keap1-KD (**B**) and
Nrf2-KO (**C**) mice. The maximal rate of complex II-dependent respiration with the highest
levels of FAD was estimated through application of the uncoupler FCCP, and the lowest
FAD levels were measured through application of the complex IV inhibitor sodium cyanide.
Each slice was placed in glucose-free HBSS, and the FAD autofluorescence was
continuously monitored at the basal state and after sequential addition of hexanoic acid (0.5
mM), followed by FCCP (1 μM) and sodium cyanide (1 mM). (**D**) FAD pool recovery rate
after addition of sodium cyanide. Data are presented as means ± S.E.M. *P < 0.05 compared
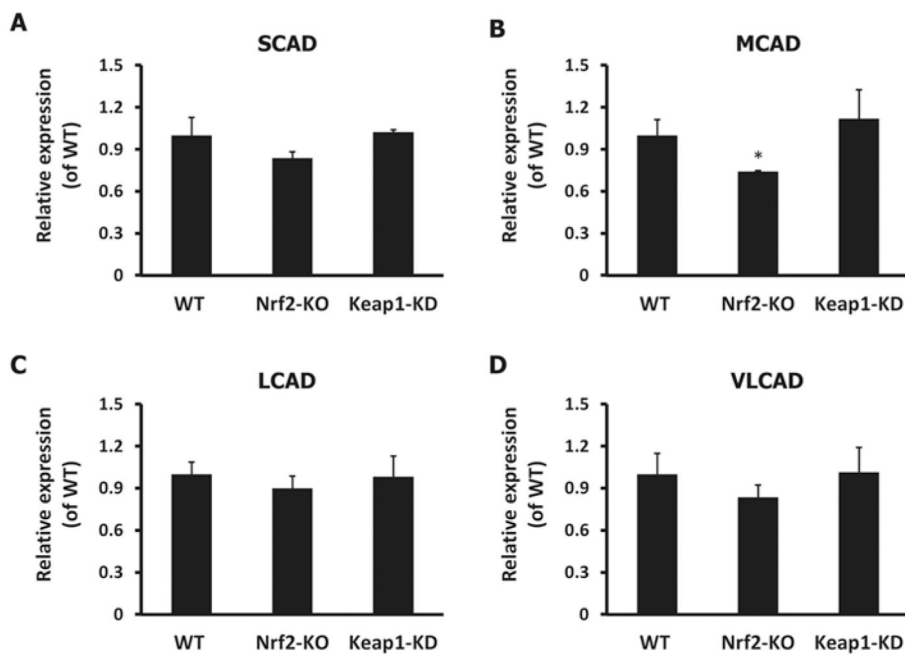with WT. NaCN, sodium cyanide.

Figure 6. Effect of Nrf2 on the transcript levels of acyl-CoA dehydrogenases
The amount of mRNA for SCADs (**A**), MCADs (**B**), LCADs (**C**) and VLCADs (**D**) were analysed by real-time PCR, using β-actin mRNA as an internal control. In each group, the mRNA species was measured separately in triplicate. Data are presented as means ± S.D. and are expressed relative to WT. *$P<0.05$ compared with WT.
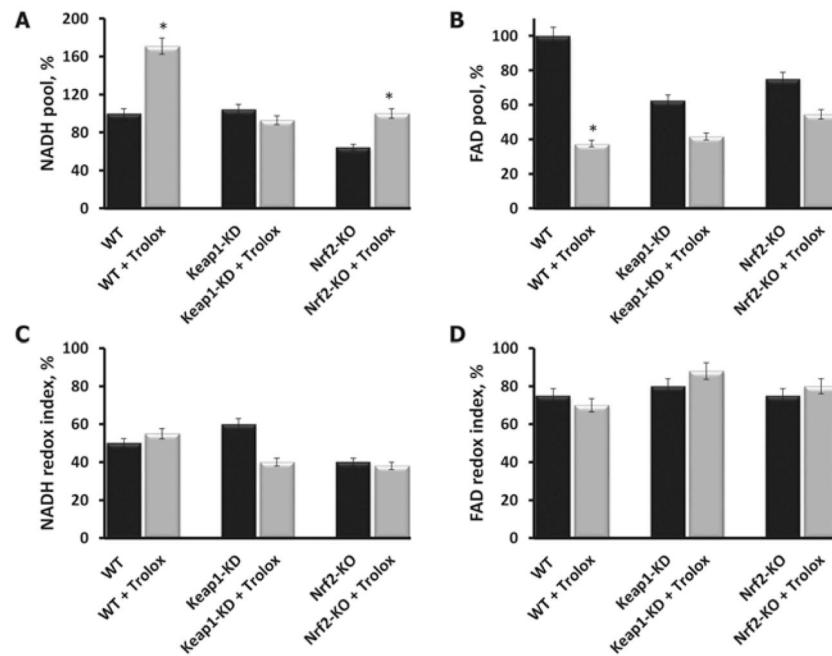
Figure 7. Effect of trolox on NADH and FAD levels and redox state

The mitochondrial NADH (**A**) and FAD (**B**) levels were determined by application of 1 μM FCCP (giving maximal values for FAD and minimal for NADH) and 1 mM sodium cyanide (giving minimal values for FAD and maximal for NADH). The redox index (**C** and **D**) is expressed as a percentage of the basal autofluorescence of NADH or FAD before application of 1 μM FCCP (taken as 0 for NADH and 100% for FAD). Parallel experiments were performed using MEFs that were pre-incubated with 100 μM trolox for 6 h or solvent control (0.1% DMSO). Data are presented as means ± S.E.M. *P<0.05 compared with control (no trolox).